J Incl Phenom Macrocycl Chem (2009) 64:121–131
DOI 10.1007/s10847-009-9544-7

ORIGINAL ARTICLE

Host–guest complexes of some cucurbit[n]urils with the hydrochloride salts of some imidazole derivatives

Yan Feng · Sai-Feng Xue · Zhi-Fang Fan · Yun-Qian Zhang · Qian-Jiang Zhu · Zhu Tao

Received: 15 November 2008 / Accepted: 17 January 2009 / Published online: 6 February 2009

Abstract Interaction between the normal cucurbit[n]urils ($n = 6,7,8$; Q[6], Q[7], Q[8]) and a sym-tetramethyl-substituted cucurbit[6]uril derivative (TMeQ[6]) with the hydrochloride salts of some imidazole derivatives N-(4-hydroxylphenyl)imidazole (g1), N-(4-aminophenyl)imidazole (g2), 2-phenylimidazole (g3) in aqueous solution was investigated by using ^{1}H NMR spectroscopy, electronic absorption spectroscopy and fluorescence spectroscopy, as well as by using a single crystal X-ray diffraction determination. The ^{1}H NMR spectra analysis established a basic interaction model in which inclusion complexes with a host:guest ratio of 1:1 forms for the Q[6]s and Q[7] cases, while with a host:guest ratio of 1:2 form for the Q[8] cases. It was common that the hosts selectively bound the phenyl moiety of the guests. Absorption spectrophotometric and fluorescence spectroscopic analysis in aqueous solution defined the stability of the host–guest inclusion complexes at pH 5.8 with a host:guest ratio of 1:1 form quantitatively as logK values between 4 and 5 for the smaller hosts Q[6 or 7]s, while with a host:guest ratio of 1:2 form quantitatively as logK values between 11 and 12 for the host Q[8]. Two single crystal X-ray structures of the inclusion complexes TMeQ[6]-g2 · HCl and TMeQ[6]-g3 · HCl showed the phenyl moiety of these two guests inserted into the host cavity, which supported particularly the ^{1}H NMR spectroscopic study in solution.

Keywords Host–guest complexes · Normal cucurbit[$n = 6,7,8$]urils · Sym-tetramethyl-cucurbit[6]uril · Imidazole derivatives · ^{1}H NMR spectroscopy · Binding constant · Crystal structure

Y. Feng · S.-F. Xue (✉) · Z.-F. Fan · Y.-Q. Zhang · Q.-J. Zhu · Z. Tao
Key Laboratory of Macrocyclic and Supramolecular Chemistry of Guizhou Province, Guizhou University, Guiyang 550025, People's Republic of China
e-mail: sfxue@gzu.edu.cn; gzutao@263.net

Introduction

A hydrophobic cavity and polar carbonyl groups surrounding the opening portals are common characteristic features for a relatively new receptor family—the cucurbit[n]uril (Q[n]) compounds. Amongst known examples, the structure of cucurbit[6]uril (Q[6]) was first determined and reported by Mock and coworkers in 1981 [1]. About two decades later, homologues cucurbit[$n = 5,7,8$]urils (Q[5], Q[7], Q[8]) were synthesized and reported by two groups in 2000 [2, 3], while cucurbit[10]uril (Q[10]), formed along with Q[5], was reported in 2002 [4]. The varying cavity and portal sizes available in Q[n] molecules, and particularly their ability to form inclusion or exclusion complexes with organic species or inorganic ions, led to quite a few researchers focusing on this area and uncovering the remarkable molecular recognition properties that provide a building block for supramolecular chemistry [5–11].

Recently, a series of Q[n] derivatives such as fully substituted cyclohexane Q[5] and Q[6] [12], a diphenyl Q[6] [13] and perhydroxycucurbit[6]uril ($(OH)_{12}$Q[6]) [14] were synthesized and reported to overcome the poor solubility of the general Q[n] family in common solvents. Using the dimer of glycoluril [15] synthesized in our laboratories and the diether of alkylglycoluril, we were able to synthesize a series of new symmetrical and unsymmetrical substituted cucurbit[n]urils [16–22]. Some Q[n] molecules show surprising water solubility, which allows us to investigate host-guest chemistry in water.

In this work, we report a series of host–guest interaction systems in which the hosts are the normal cucurbit[n]urils

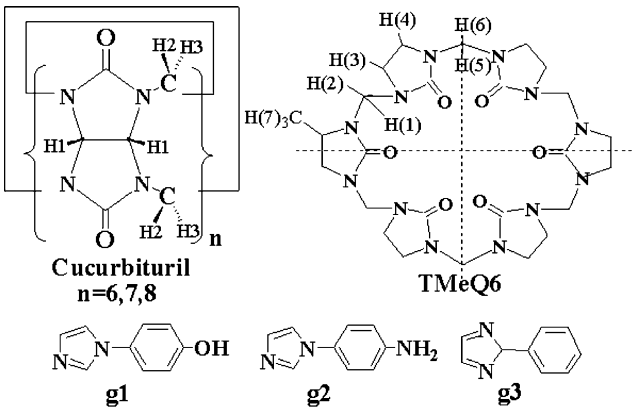

Fig. 1 Structures of cucurbit[*n*]urils and the related guests

(n = 6,7,8, marked Q[6], Q[7], Q[8]) and a water soluble symmetrically tetramethyl-substituted cucurbit[6]uril (marked TMeQ[6]) [16] and the guests are the hydrochloride salts of N-(4-hydroxylphenyl)imidazole (g1), N-(4-aminophenyl)imidazole (g2), 2-phenylimidazole (g3) (referring to Fig. 1). These guests are composed of two unsaturated moieties—phenyl and imidazole rings—both of which are sufficiently small that they could be included in the cavity of the selected hosts or its substituted derivatives [23–27]. ^{1}H NMR spectroscopy and a single crystal X-ray diffraction determination reveal that the inclusion complex formed has an unsymmetrical configuration with the phenyl moiety being the included moiety of the guests, and the imidazole moiety of the guests being the excluded moieties, the configurations proved recently exhibiting efficient cleavage of some DNA in physiological environment [28]. The stability of this complex has been estimated by using electronic absorption spectroscopy and fluorescence spectroscopy methods. Results of this study are reported herein.

Experimental

Materials

Cucurbit[6–8]uril were prepared and purified in our laboratories according to the literature method [2, 3]. TMeQ[6] was prepared and purified according to the method developed in our laboratories [16]. N-(4-hydroxylphenyl)imidazole (g1), N-(4-aminophenyl)imidazole (g2), 2-phenylimidazole (g3) was obtained from Aldrich and used without further purification. The corresponding HCl salts were prepared by dissolving the related guests in 5 M HCl followed by crystallization after ethanol addition, collecting the crystals by filtration and drying in air, respectively.

The single crystals of TMeQ[6] adduct with g2 · HCl and g3 · HCl were obtained by dissolving TMeQ[6] (0.20 g, 0.19 mmol) in a solution of g2 or g3 · HCl (0.046 and 0.036 g, 0.20 mmol) in water (5 mL). The final solution was mixed thoroughly and allowed to stand at room temperature; crystals formed after several days, and were collected.

Host–guest complexation

For the study of host-guest complexation of the related host Q[n] or TMeQ[6] and the guests, 2.0–2.5 × 10^{-3} mmol samples of Q[n] in 0.5–0.7 g D_2O with guest: Q[7] or TMeQ[6] ratios ranging between 1 and 100 were prepared. The ^{1}H NMR spectra were recorded at 20 °C on a Varian INOVA-400 spectrometer. The pD of the solution was ~5.7.

Absorption spectra of the host–guest complex were recorded on a HP8453 UV-visible spectrophotometer and fluorescence spectra of the host–guest complexes were recorded on a Varian RF-540 fluorescence spectrophotometer at room temperature. For absorption and fluorescence studies, aqueous solutions of the guest · HCl were prepared with a fixed concentration of 3.20 × 10^{-5} mol L^{-1}, and the samples of these solutions were combined with Q[n]s or TMeQ[6] to give solutions with a guest : Q[n] ratio of 0:10, 1:9, 2:8, …, 9:1, 10:0, respectively. The pH of the solution was ~5.7.

X-ray crystallography

A Bruker SMART ApexII CCD diffractometer employing graphite monochromated MoKα radiation was used for the data collection. A suitable crystal of TMeQ[6]-g2 or g3 · HCl were selected and mounted at the end of a glass fiber. Data were collected at 223(2) Kelvin with ϕ and ω scans. No crystal decay was observed. Data integration and reduction and subsequent computations were carried out with the Bruker ApexII package, including Lorentz polarization and absorption correction. The structure was solved by direct methods with SHELXS-97, and extended and refined with SHELEL-97 [29]. Hydrogen atoms were added at calculated positions and refined using a riding model; solvent H-atoms were not usually located. Anisotropic displacement parameters were used for all non-H atoms; H-atoms were given isotropic displacement parameters equal to 1.2 (or 1.5 for methyl hydrogen atoms) times the equivalent isotropic displacement parameter of the atom to which the H-atom is attached. Residuals are defined as $R1 = \Sigma||F_o| - |F_c||/\Sigma|F_o|$ for $F_o > 2\sigma(F_o)$ and $wR2 = [\Sigma w(F_o^2 - F_c^2)^2/\Sigma(wF_c^2)^2]^{1/2}$ for all reflections, with $w = 1/[\sigma^2(F_o^2) + (AP)^2 + BP]$ where $P = (F_o^2 + 2F_c^2)/3$ and A and B are given below.

TMeQ[6]-g2 · HCl. Formula $C_{49}H_{89}ClN_{27}O_{30}$, M = 1571.92, monoclinic, space group $P/(C2/m)$, a = 14.678(3) Å, b = 18.795(3) Å, c = 12.977(2) Å, α = 90.00°,

$\beta = 95.846°$, $\gamma = 90.00°$, $V = 3561.5$ Å^3, $D_c = 1.466$ g cm^{-3}, $Z = 2$, crystal size 0.10 by 0.11 by 0.18 mm, colourless, prism, temperature 223(2) Kelvin, λ(MoKα) 0.71073 Å, μ(MoKα) 0.1587 mm^{-1}, $F_{000} = 1658$, $R1 = 0.1305$, $Rw = 0.3721$, $T_{min,\ max}$ 0.9722; 0.9844. Range of θ 1.77–25.00°. *hkl* range −17 17, −22 21, −15 15, N 3206, N_{ind} 2337 (R_{int} 0.0283), restraints 21, parameters 305, N_{obs} 3206 ($I > 2\sigma(I)$). Residuals *R1(F)* [for 3206 reflections with $I > 2\sigma(I)$] 0.1523, *wR2*(F^2) 0.4003 for $A = 0.2000$ and $B = 0.0000$. GoF(all) 1.738, $\Delta\rho_{\min,\ \max}$ −1.123, 1.294 e$^-$ Å^{-3}.

TMeQ[6]-g3 · HCl. Formula $C_{49}H_{99}ClN_{26}O_{35}$, $M = 1647.99$, triclinic, space group *P - 1*, $a = 12.1844(13)$ Å, $b = 12.8088(14)$ Å, $c = 23.441(3)$ Å, $\alpha = 90.016°$, $\beta = 102.2460°$, $\gamma = 91.9840°$, $V = 3572.9$ Å^3, $Dc = 1.532$ g cm^{-3}, $Z = 2$, crystal size 0.15 by 0.13 by 0.16 mm, colourless, prism, temperature 223(2) Kelvin, λ(MoKα) 0.71073 Å, μ(MoKα) 0.165 mm^{-1}, $F_{000} = 1744$, $R1 = 0.0787$, $Rw = 0.2350$, $T_{min,\ max}$ 0.9741; 0.9788. Range of θ 0.89–25.00°. *hkl* range −14 14, −15 14, −27 27, N 12194, N_{ind} 9351(R_{int} 0.0207), restraints 0, parameters 1008, N_{obs} 12194 ($I > 2\sigma(I)$). Residuals *R1(F)* [for 12194 reflections with $I > 2\sigma(I)$] 0.0955, *wR2*(F^2) 0.2469 for $A = 0.1378$ and $B = 5.7558$. GoF(all) 1.054, $\Delta\rho_{\min,\ \max}$ −0.880, 0.821 e$^-$ Å^{-3}.

Views of the complexes appear in Fig. 10a, b and c, d. Crystallographic data (excluding structure factors) for the structure reported have been deposited with the Cambridge Crystallographic Data Centre as supplementary publication no. CCDC-707624 and CCDC-707625. Copies of the data can be obtained free of charge on application to CCDC, 12 Union Road, Cambridge CB2 1EZ, UK [Fax: (internat. + 44-1223/336-033; E-mail: deposit@ccdc.cam.ac.uk].

Results and discussion

The interaction of a host and guest to form an inclusion complex commonly causes a change in the environment of the guest that is sufficient to be monitored by spectroscopic methods. Often, water solubility of one or both species is problematical, such as in the cases involving with Q[6] or Q[8], in which the solubility of the hosts was limited. Thus, the water soluble TMeQ[6] was used for replacing the normal Q[6] in ^{1}H NMR determination, and electronic absorption spectroscopy or fluorescence spectroscopy was used for studying host–guest complexation.

^{1}H NMR spectra analysis of the interaction between the Q[n]s with g1 · HCl

Figure 2 shows the ^{1}H NMR spectra of g1 · HCl recorded in the absence and in the presence of 0.25 equivalent of Q[6], 1.10 equivalent of Q[7] and 0.44 equivalent of Q[8]. One can see that the guest shows broadening of the proton signals, indicating average to fast exchange, and the proton signals of the water insoluble host Q[6] suggest that the host Q[6] interacts with the guest g1 · HCl (Fig. 2a, b). However, it is hard to decide the interaction details due to no obvious upfield or downfield shifts of the guest proton.

Signals corresponding to the bound g1 · HCl are present after addition of 1.1 equivalents of Q[7] (Fig. 2c). All guest resonances are shifted upfield by 0.21 (for H^5), 0.16 (for H^4) and 0.02 ppm (for H^3), particularly, significant upfield by 0.96 (for H^1) and 0.99 ppm (for H^2). This suggests that the whole guest molecule is in the shielding zone in the cavity of the host and the phenyl ring of the guest is much deeper in the cavity of the host. The sharp peaks of the bound g1 · HCl indicate that exchange between the included and excluded guest is slow on the NMR time scale. Both signals corresponding to the bound g1 · HCl and the water insoluble host Q[8] are present after addition of 0.45 equivalents of Q[8] (Fig. 1d). Similar to the Q[7]-g1 system, all guest resonances are shifted upfield by 0.33 (for H^5), 0.26 (for H^4) and 0.10 ppm (for H^3), particularly, significant upfield by 1.12 (for H^1) and 1.06 ppm (for H^2). This suggests that the whole guest molecule also is in the shielding zone in the cavity of the host and the phenyl ring of the guest is much deeper in the cavity of the host. However, the significant broadening peaks of the bound g1 · HCl indicate that exchange between the included and excluded guest is much faster on the NMR time scale. Moreover, a comparison of the integrals of the protons of the bound g1 · HCl with the protons of Q[8] revealed to be 1:2 of host : guest.

To understand the interaction details between Q[6] with g1 · HCl, a water soluble host, TMeQ[6] was used for investigating the interaction with the guest g1 · HCl. Figure 3 shows the ^{1}H NMR spectra of g1 · HCl recorded in

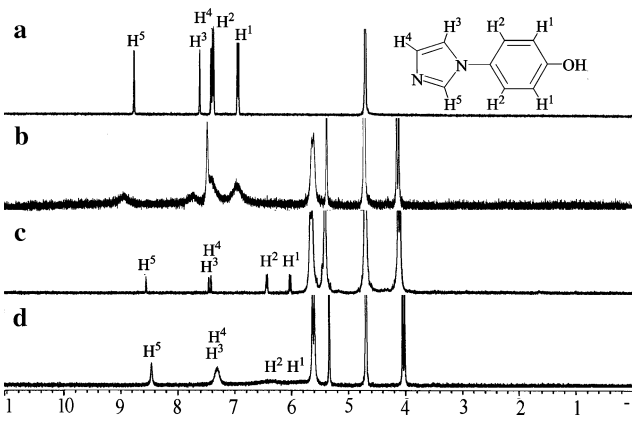

Fig. 2 The ^{1}H NMR spectra of g1 · HCl recorded **a** in the absence and **b** in the presence of 0.25 equivalent of Q[6], **c** 1.10 equivalent of Q[7] and **d** 0.44 equivalent of Q[8]

the absence and in the presence of up to 2.1 equivalents of TMeQ[6], as well as that of neat TMeQ[6]. Signals corresponding to the unbound and bound g1 · HCl are present after addition of 1.2 equivalents of TMeQ[6] (Fig. 3a, b), with the signals of the unbound guest almost disappearing when the concentration of TMeQ[6] reaches 2.1 equivalents (Fig. 3c). Two phenyl ring resonances are shifted significantly upfield by 1.08 (for $H^{1'}$), 0.56 (for $H^{2'}$), while two of imidazole ring resonances are shifted significantly downfield by 0.95 (for $H^{5'}$), 0.82 (for $H^{3'}$). This suggests that the phenyl ring of the guest is in the shielding zone in the cavity of the host, while the imidazole ring is in the deshielding zone at the portal of the host. The broadening peaks of the bound g1 · HCl indicate that exchange between the included and excluded guest is fast on the NMR time scale.

For the TMeQ[6] host, the resonances of the protons H(1), H(2) and H(7) in the inclusion complex show no obvious shift, whereas the resonances of the protons H(3), H(4), H(5), and H(6) experience not only an upfield shift, but also split into two sets compared to the free TMeQ[6] (Fig. 2c, d). The overlapped resonances of the protons H(3), H(4) are displaced by an upfield shift by ~0.2 ppm (marked H(3)′) and ~0.4 ppm (marked H(4)′), respectively, and both H(5) and H(6) are broaden and shifted upfield with splitting by 0.2–0.3 ppm (marked H(5)′ and H(6)′), and 0.4–0.5 ppm (marked H(5)″ and H(6)″) for each pair. The two sets of split doublet resonances of H(5) and H(6) show that the two protons on the portal methylenes of the TMeQ[6] lie in different magnetic environments, caused by a preferential orientation of the protruding imidazole of the guest g1 · HCl towards one portal of TMeQ[6]. Thus, the ^{1}H NMR study strongly implies that TMeQ[6] exhibits a pronounced preference towards including the phenyl moiety rather than the imidazole moiety of g1 · HCl [22], with the structure of the inclusion complex being unsymmetrical.

^{1}H NMR spectra analysis of the interaction between the Q[n]s with g2 · HCl

Figure 4 shows the ^{1}H NMR spectra of g2 · HCl recorded in the absence and in the presence of 0.30 equivalent of Q[6], 0.25 equivalent of TMeQ[6], 1.10 equivalent of TMeQ[6], 0.94 equivalent of Q[7] and 0.48 equivalent of Q[8]. For the cases of Q[6]-g2 · HCl and TMeQ[6]-g2 · HCl, the ^{1}H NMR spectra present similar results that the signals of the bound g2 · HCl are present besides the excess unbound guest (Fig. 4a, b, c). Two phenyl ring resonances are shifted significantly upfield by 0.94 (for $H^{1'}$), 0.71 (for $H^{2'}$), and a resonance of imidazole proton, which can be observed clearly in Fig. 4d, is also shifted upfield by 0.21 (for $H^{4'}$), while the rest two of imidazole ring resonances are shifted significantly downfield by 0.81 (for $H^{5'}$), 0.83 (for $H^{3'}$). This suggests that the phenyl ring of the guest is in the shielding zone in the cavity of the host, while the imidazole ring is in the deshielding zone at the portal of the host. This conclusion was further proved by the crystal structure of the inclusion complex of TMeQ[6]-g2 · HCl.

Signals corresponding to the bound g2 · HCl are present after addition of 0.94 equivalents of Q[7] (Fig. 4e). The upfield shifts of the guest resonances of the guest indicate that the whole guest is in the shielding zone. The significant upfield shift of the phenyl proton by 0.70 (for $H^{1'}$) and 0.90 ppm (for $H^{2'}$) compared to the moderate upfield shift

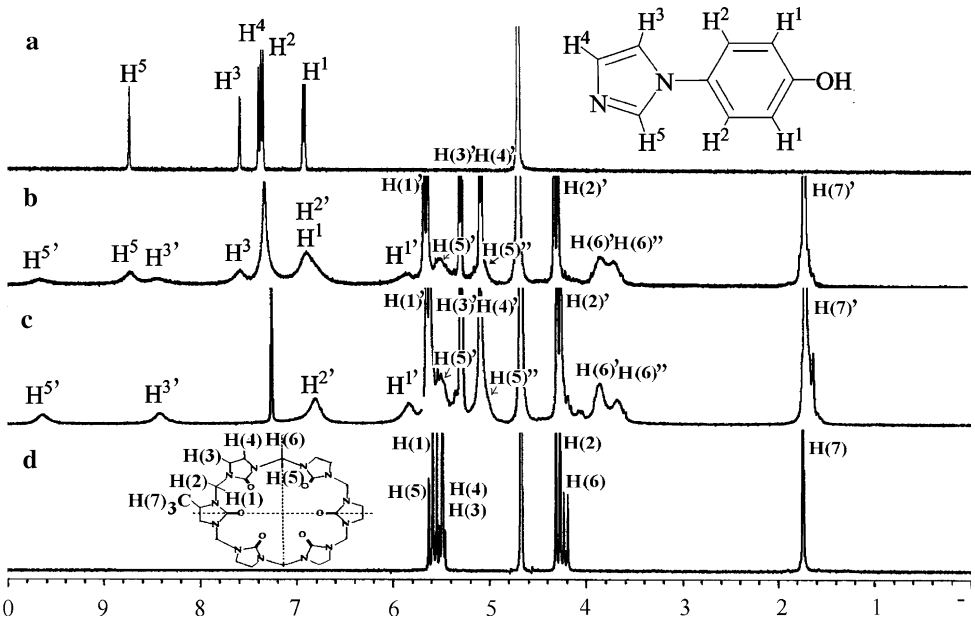

Fig. 3 ^{1}H NMR spectra of g1 · HCl recorded **a** in the absence and **b**, **c** in the presence of 0.7, 2.1 equivalents of TMeQ[6], as well as that of **d** neat TMeQ[6]

of imidazole protons by 0.51 (for $H^{5'}$), 0.18 (for $H^{4'}$) and 0.18 ppm (for $H^{3'}$) suggest that the phenyl ring of the guest is much deeper in the cavity of the host.

It is noticeable that the two sets of split doublet resonances of the portal methylene protons, for Q[6], the proton H2 and H3 referring to Fig. 1, and for TMeQ[6], the protons H(5) and H(6) referring to Fig. 3, reveal that the protons on the portal methylenes of these hosts lie in different magnetic environments, caused by a preferential orientation of the imidazole moiety of the guest g2 · HCl towards one portal of the above mentioned hosts. For the bound Q[6], the doublet resonance of H2 split obviously into two sets broadening doublet resonances, while the doublet resonances of H3 split slightly, and give a triplet resonances (referring to Fig. 4b). For the bound TMeQ[6], the situation similar to the TMeQ[6]-g1 · HCl system, both H(5) and H(6) are broaden and shifted upfield with splitting by 0.15–0.25 ppm (H(5)′ and H(6)′), and 0.45 ppm (H(5)″ and H(6)″) for each pair. Moreover, the overlapped resonances of the protons H(3), H(4) are displaced by an upfield shift by ∼0.2 ppm (H(3)′) and ∼0.4 ppm (H(4)′), respectively. A comparison of the integrals of the shifted protons of the bound g2 · HCl with the shifted protons of the hosts revealed the inclusion complex to be a 1:1 host:guest species. Thus, the ^{1}H NMR study also strongly implies that Q[6] and TMeQ[6] exhibit a preference towards including the phenyl moiety rather than the imidazole moiety of g2 · HCl, with the structure of the inclusion complex being unsymmetrical.

Both signals corresponding to the bound g2 · HCl and Q[7] or the water insoluble host Q[8] are present after addition of 0.48 equivalents of Q[8] (Fig. 4e, f), and the different upfield shifts of protons of the included guest (imidazole protons by 0.32–0.43 ppm; phenyl protons by 1.22–1.29 ppm) suggest that the phenyl ring of the guest is much deeper in the cavity of the host. A comparison of the integrals of the protons of the bound g2 · HCl with the protons of Q[7] and Q[8] revealed to be 1:1 and 1:2 of host:guest species, respectively.

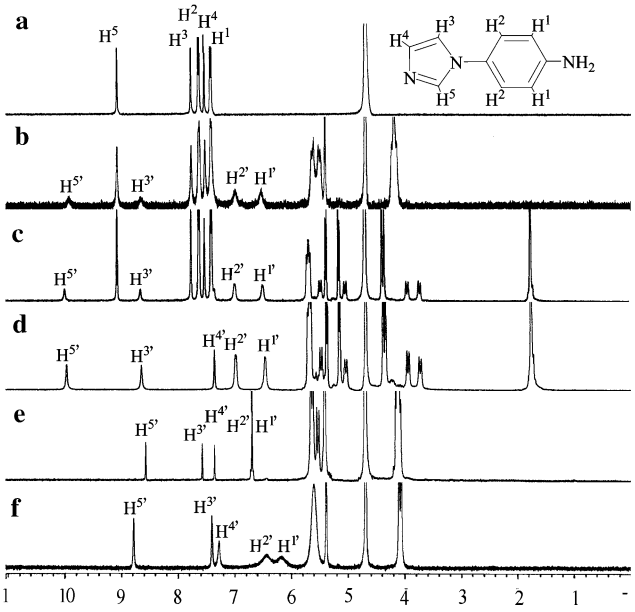

Fig. 4 The ^{1}H NMR spectra of g2 · HCl recorded **a** in the absence and **b** in the presence of 0.30 equivalent of Q[6], **c** and **d** 0.25 and 1.05 equivalent of TMeQ[6], **e** 0.94 equivalent of Q[7] and **f** 0.48 equivalent of Q[8]

Unlike the other three Q[n]-g2 · HCl systems, the two sets of doublet resonances of the portal methylene protons H2 and H3 do not split, except the resonance of H2 become broaden in the Q[8]-g2 · HCl system. In our previous work, we have demonstrated some samples that Q[8] included two small organic molecules in two typical styles: the guest pair protrudes from the same portal of the host Q[8] to form an unsymmetrical inclusion complex [30, 31] or from the opposite portals of the host to form a symmetrical inclusion complex [32]. Above ^{1}H NMR study for the Q[8]-g2 · HCl system implies that Q[8] includes the phenyl moiety much deeper than the imidazole moiety of two g2 · HCl guest, and the protruding pyrazole moieties of the two bound guest g2 · HCl towards both portals of Q[8] with the structure of the inclusion complex being symmetrical.

^{1}H NMR spectra analysis of the interaction between the Q[n]s with g3 · HCl

The Q[n]s-g3 · HCl systems presented similar host-guest interaction results to the Q[n]s-g1 or g2 · HCl systems. The upfield shifts (between 0.38 and 0.9 ppm) of the phenyl proton resonances of the bound g3 · HCl and the downfield shifts (about 0.3 ppm) of imidazole protons resonances of the bound g3 · HCl in Q[6]-g3 · HCl, TMeQ[6]-g3 · HCl and Q[7]-g3 · HCl systems (Fig. 5b, c, d) revealed that the hosts showed a preference towards including the phenyl moiety of g3 · HCl, also the split doublet of H2 of the portal methylene protons of the host Q[6] or Q[7], as well the split doublet of H(5) and H(6) of the portal methylene protons of the host TMeQ[6] further confirmed the structure of the inclusion complex being unsymmetrical. For the Q[8]-g3 · HCl system, although the resonances of the host Q[8] was observed, the resonances of the bound guest were too vaguer to be observed, even the ratio of guest:host was up to 20:1(Fig. 5e). The solubility of the host and the host–guest inclusion complex could be the reason, and the interaction between Q[8] and g3 · HCl will be discussed late.

Spectrophotometric analysis on the interaction between Q[n]s and g · HCl

To further quantify the interaction between the Q[n]s and g1–3 · HCl, a ratio-dependent study was pursued by

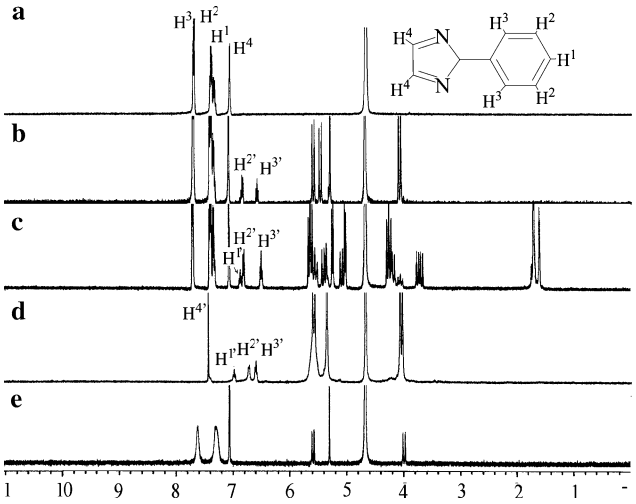

Fig. 5 The ^{1}H NMR spectra of g3 · HCl recorded **a** in the absence and **b** in the presence of 0.10 equivalent of Q[6], **c** 1.25 equivalent TMeQ[6], **d** 1.10 equivalent of Q[7] and **e** 0.05 equivalent of Q[8]

electronic absorption and fluorescence spectra at pH 5.8. Usually, all four free hosts Q[n]s show no absorbance at $\lambda > 210$ nm, and the three free g1–3 · HCl show the maximum absorption at λ_{max} 239 nm for g1 · HCl, 255 nm for g2 · HCl, 262 nm for g3 · HCl, respectively.

Figure 6a–c show the variation in the UV spectra obtained with aqueous solutions containing a fixed concentration of g1–3 · HCl (32 mM) and variable concentrations of Q[6], respectively. The absorption band of the guests exhibits a progressively lower absorbance with a red shift as the ratio of $N_{Q[6]}/N_{g\cdot HCl}$ is increased. The absorbance (A) *vs* ratio of moles of the host Q[6] and guests ($N_{Q[6]}/N_{g\cdot HCl}$) data can be fitted to a 1:1 binding model for all the three Q[6]-g · HCl systems at λ_{max}, respectively (Fig. 6d). This behaviour is consistent with the results from the ^{1}H NMR study.

For the three TMeQ[6]-g1–3 · HCl systems, The absorption band of the guests exhibits a progressively lower absorbance with a red shift as the ratio of $N_{TMeQ[6]}/N_{g\cdot HCl}$ is increased, and a sharp isosbestic point at 249 nm for TMeQ[6]-g1 · HCl system, and 262 nm for TMeQ[6]-g2 · HCl system further confirms a simple interaction between TMeQ[6] and the selected guests, respectively (referring to Fig. 7a–c). The absorbance (A) versus ratio of moles of the host TMeQ[6] and guests ($N_{TMeQ[6]}/N_{g\cdot HCl}$) data can be fitted to a 1:1 binding model for all the three TMeQ[6]-g · HCl systems at λ_{max}, respectively (Fig. 7d).

For the three Q[7]-g · HCl and Q[8]-g · HCl systems, the absorption bands of the guests show a similar tendency and exhibit a progressively lower absorbance as the ratio of $N_{Q[n]}/N_{g\cdot HCl}$ is increased (Fig. 8a–c and e–g), however, the absorbance (A) *versus* ratio of moles of the host Q[7] and guests ($N_{Q[7]}/N_{g\cdot HCl}$) data can be fitted to a 1:1 binding model at the corresponding λ_{max}, while the absorbance (A) *versus* ratio of moles of the host Q[8] and guests ($N_{Q[8]}/N_{g\cdot HCl}$) data can be fitted to a 1:2 binding model at the corresponding λ_{max} (Fig. 8d, h). The absorbance change

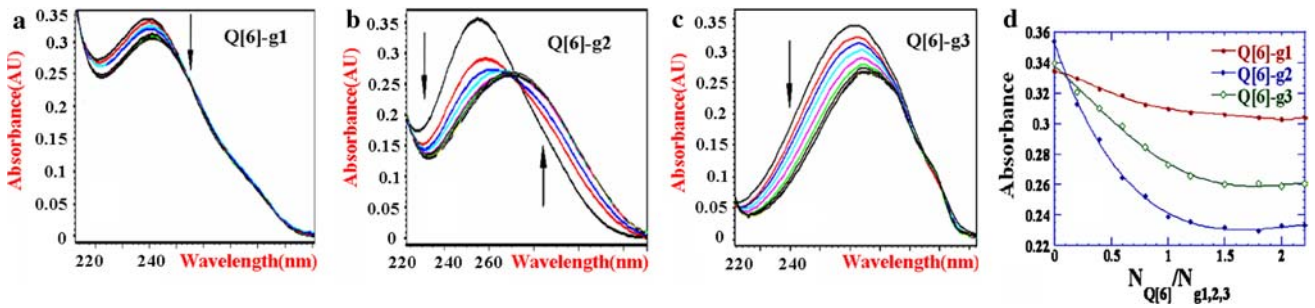

Fig. 6 Electronic absorption spectra and corresponding A ~ $N_{Q[6]}/N_{g1-3}$ curves

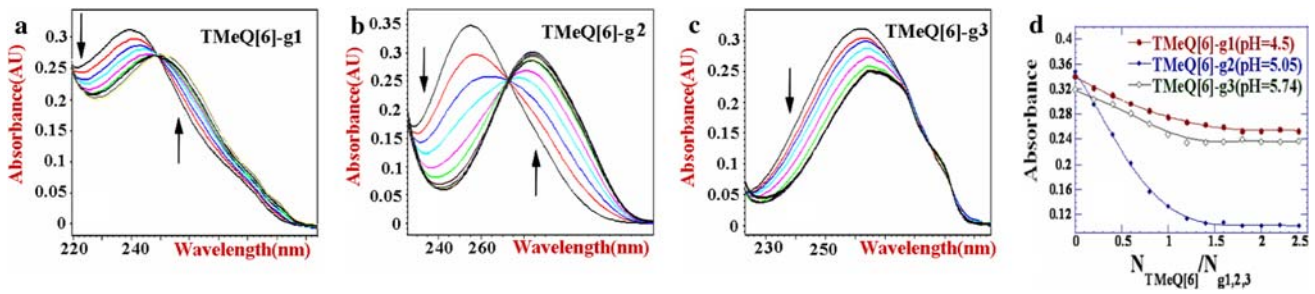

Fig. 7 Electronic absorption spectrum and corresponding A ~ $N_{TMe[6]}/N_{g1,2,3}$ curves

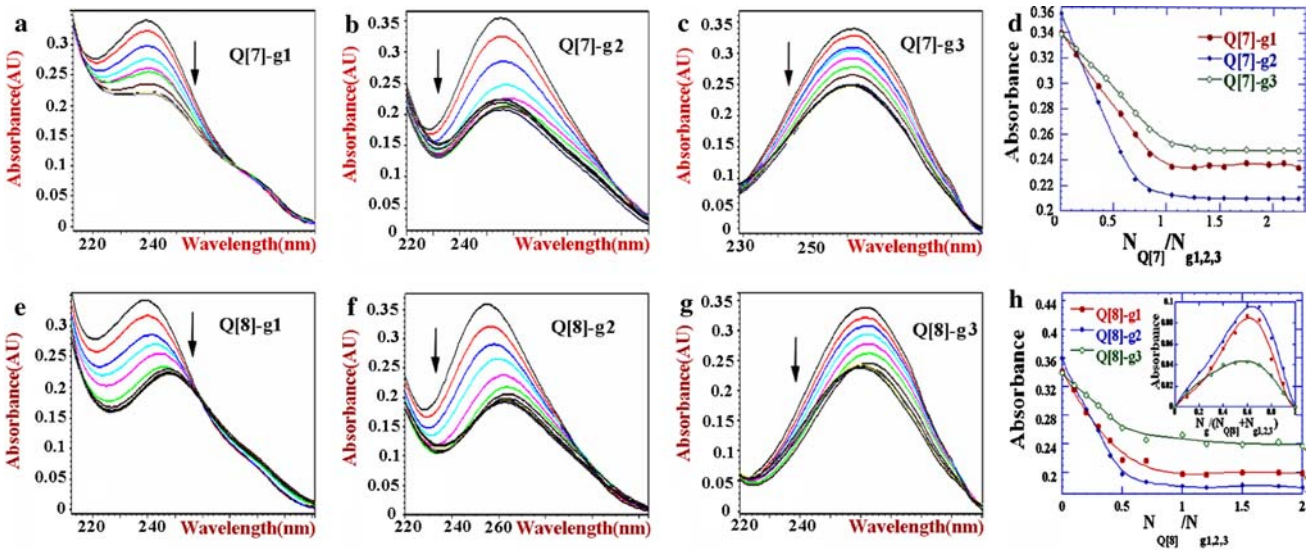

Fig. 8 Electronic absorption spectrum and corresponding A ~ $N_{Q[7]}/N_{g1,2,3}$curves

(ΔA) *vs* ratio of $[N_{TMeQ[6]}/(N_{TMeQ[6]} + N_{g\cdot HCl})]$ data also confirm that the interaction between Q[8] with the selected guests can be fitted to a 1:2 binding model.

Fluorescence spectroscopy, similar experiments were performed. All four free hosts Q[n]s were non-fluorescence materials and the maximum fluorescence emission wavelength of the three selected guests g1–3 · HCl were 321, 365 and 321 nm, respectively. The fluorescence of the guests g1 · HCl and g2 · HCl was found to increase with the increase in the two Q[6]s (Q[6] and TMeQ[6]) concentration at 398, 424 nm, respectively, while the fluorescence of these two guests were almost completely quenched with the increase in the host Q[7] or Q[8] concentration. For the g3 · HCl, its fluorescence intensity was always decreased with the increase in the hosts concentration (referring to Fig. 9). For the nine Q[6]-g1–3 · HCl, TMeQ[6]-g1–3 · HCl and Q[7]-g1–3 · HCl systems, the all curves of fluorescence intensity (If) *vs* $N_{Q[n]}/N_{g\cdot HCl}$ can be fitted to a 1:1 binding model. For the three Q[8]-g1–3 · HCl systems, the curves of fluorescence intensity (If) *vs* $N_{Q[n]}/N_{g\cdot HCl}$ and ΔIf *versus* $[N_{TMeQ[6]}/(N_{TMeQ[6]} + N_{g\cdot HCl})]$ can be fitted to a 1:2 binding model (Fig. 9).

The measured data from both absorption spectrophotometric analysis (ASA) and fluorescence spectroscopy analysis (FSA) for the twelve inclusion host–guest systems yielded calculated binding constants (K), the corresponding logKs are listed in Table 1.

Crystal structure determination of the inclusion complex TMeQ[6]-g2 and g3 · HCl

Based on the solution studies, one can conclude that the hosts prefer to include the phenyl moiety rather than the imdazole moiety of the guests. The crystal structures of the inclusion complexes could give more details on the interaction between the Q[n]s hosts and the g · HCl guests. In this work, only two single crystal X-ray structures of the inclusion complexes TMeQ[6]-g2 and TMeQ[6]-g3 were obtained, both of them showed the phenyl moiety of these two guests inserted into the host cavity, which supports particularly the ^{1}H NMR spectroscopic study in solution.

Figure 10 shows the views of the TMeQ[6]-g2 · HCl and TMeQ[6]-g3 · HCl adducts. In the solid state, the phenyl moiety of the guest has clearly intruded into the cavity center of the host, whereas the imidazole moiety lies in a portal zone of the host. Thus, the phenyl ring in the cavity will undergo a shielding effect, and the corresponding proton resonances will experience a significant upfield shift (as observed in the ^{1}H NMR spectra discussed above). Moreover, the portal hydrogen bonds of the protonated imidazole moiety of the guests with the rimmed carbonyls of TMeQ[6] increased the stability of the title inclusion complexes (although it is unclear which N of the imidazole moiety is protonated in solution).

It is notable that a preferential orientation of g2 · HCl or g3 · HCl protruding from the portal of TMeQ[6] will cause a significant chemical shift difference for the protons H(5)/H(6) and H(1)/H(2). This preferential orientation favors C–H···π interaction between the phenyl ring and the protons H(5)/H(6) [33–35], which leads to an obvious upfield shift of the H(5) and H(6) signals. In addition, the location of the bound g2 · HCl or g3 · HCl favours C–H···π interaction between not only the phenyl ring but also the imidazole ring and the protons H(5)″ or H(6)″ (upper fringe of the TMeQ[6]), while the H(5)′ or H(6)′ (lower fringe of the TMeQ[6]) experience interaction with the phenyl ring only. Consequently, the H(5) and H(6) signals are further split into two sets (H(5)′/H(5)″ and H(6)′/

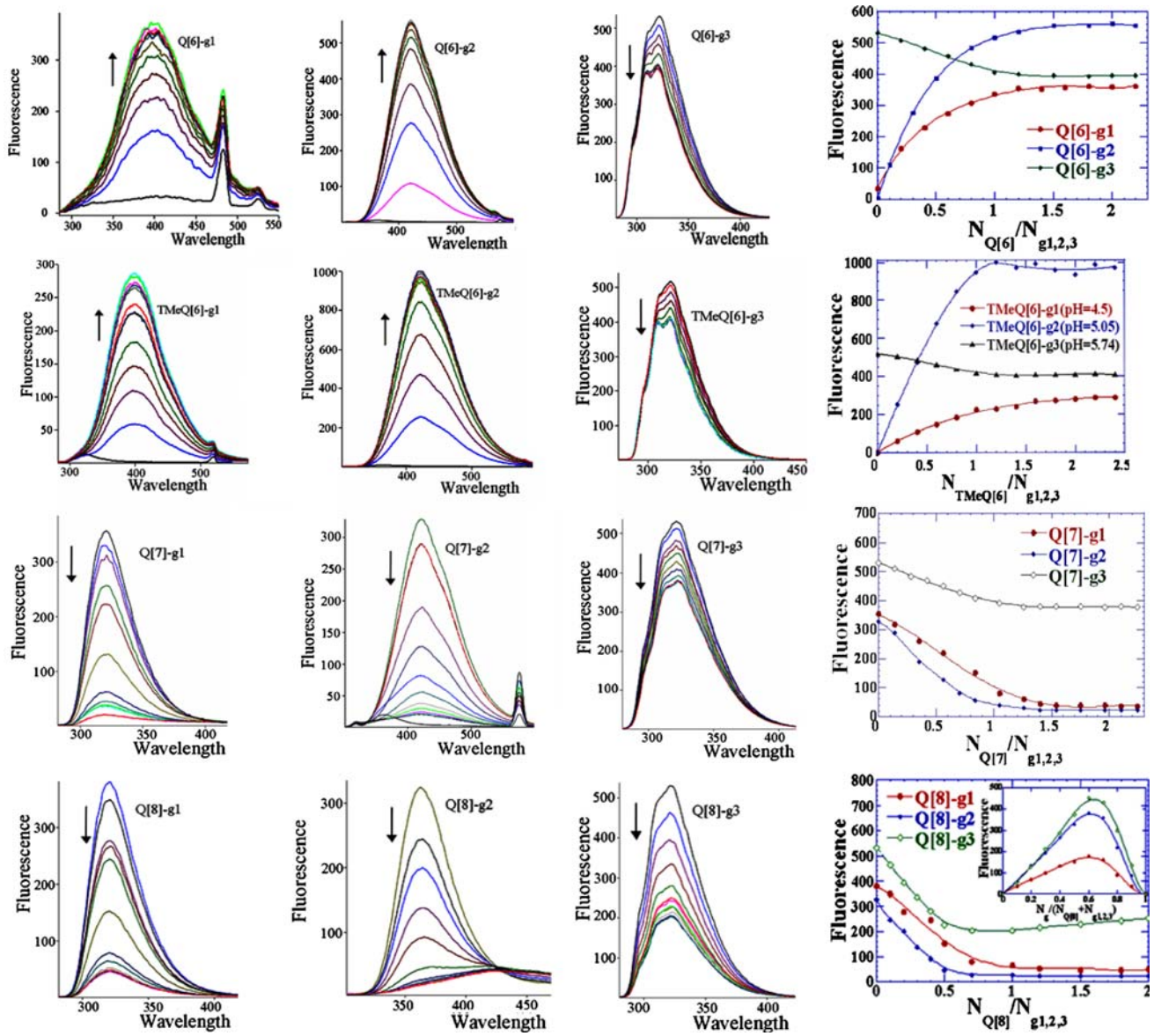

Fig. 9 Fluorescence emission spectra and corresponding If-$N_{Q[n]}/N_g$ curves and $\Delta If \sim N_g/(N_{Q[8]} + N_g)$ curves

Table 1 The binding constants (K) of the Q[n]-gn systems

Host–guest interaction ratio	Host	g1 · HCl		g2 · HCl		g3 · HCl	
		$logK_{ASA} \pm$ error	$logK_{FSA} \pm$ error	$logK_{ASA} \pm$ error	$logK_{FSA} \pm$ error	$logK_{ASA} \pm$ error	$logK_{FSA} \pm$ error
1:1	Q[6]	4.1 ± 0.1	4.3 ± 0.1	5.0 ± 0.1	4.9 ± 0.1	4.8 ± 0.1	4.6 ± 0.2
1:1	TMeQ[6]	4.9 ± 0.1	4.3 ± 0.2	4.6 ± 0.1	4.1 ± 0.1	4.8 ± 0.1	4.8 ± 0.3
1:1	Q[7]	4.9 ± 0.2	4.9 ± 0.2	4.9 ± 0.1	4.9 ± 0.1	4.7 ± 0.1	4.7 ± 0.1
1:2	Q[8]	11.8 ± 0.1	12.0 ± 0.2	11.8 ± 0.1	11.9 ± 0.1	11.1 ± 0.1	12.4 ± 0.2

H(6)″) due to their experiencing different shielding effects.

In the solid state of TMeQ[6]-g2 · HCl, the guest is inserted to the extent that the aromatic ring sits exactly in line with opposite sets of the portal carbonyl oxygens O3 and O4. The closest contacts are between the amine cation (N30) of the imidazole ring and carbonyl atoms (O1, O2, O3 and O4) of the cucurbituril, with N30…O1, N30…O2, N30…O3 and N30…O4 of 3.318, 3.465, 3.888 and 3.868 Å, respectively (Fig. 10a, b); In the solid state of TMeQ[6]-

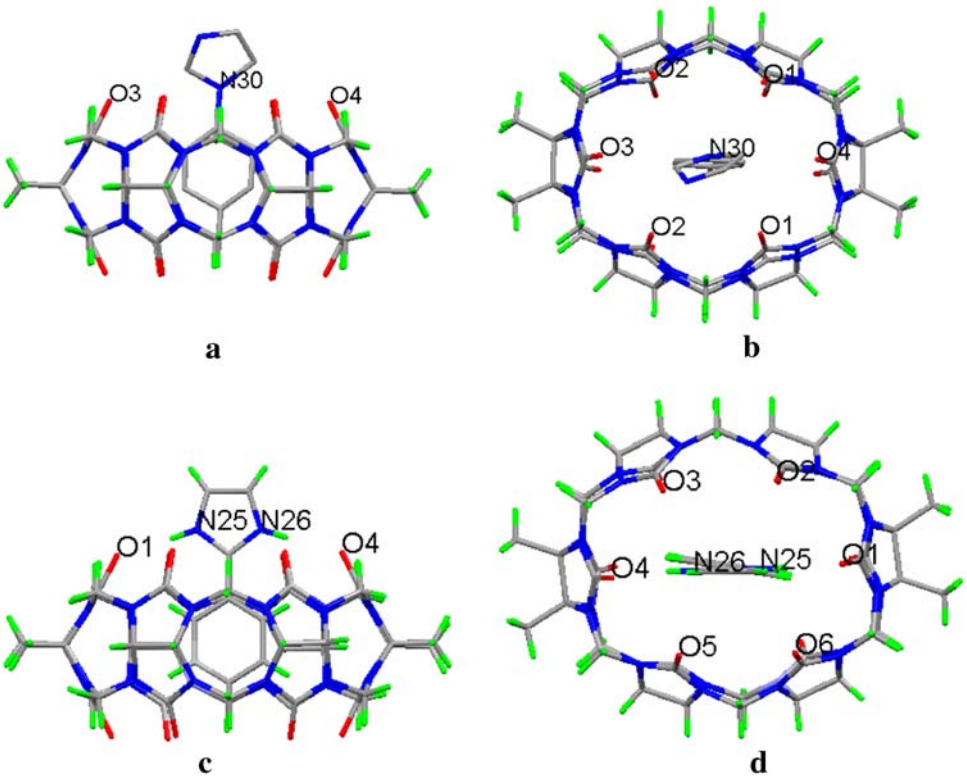

Fig. 10 Crystal structure of the inclusion complexes TMeQ[6]-g2 · HCl **a** side view, **b** top view; TMeQ[6]-g3 · HCl: **c** side view, **d** top view

g3 · HCl, the guest is also inserted to the extent that the phenyl ring sits essentially in line with opposite sets of the portal carbonyl oxygens O1 and O4, but is twisted away from linearity by 11.09°, while the phenyl is exactly in line with opposite sets of the portal carbonyl oxygens O1 and O4. The closest contacts are between the protonated secondary amine of the imidazole ring (N25 or N26) and carbonyl atoms (O1, O2, O3, O4, O5, O6) of the host TMeQ[6], with N25…O1, N25…O2, N25…O6, N26…O3, N26…O4 and N26…O5 of 2.800, 3.011, 3.082, 2.925, 2.826 and 2.958 Å; N82…O3, N82…O4 and N82…O5 of 2.923, 2.827 and 2.958 Å; respectively. The H25…O1, H25…O2, H25…O6, H26…O3, H26…O4 and H26…O5 distances are 1.940, 2.888, 2.853, 2.707, 1.969, 2.840 Å, respectively (Fig. 10c, d), for example, indicative of the strong hydrogen bonding assisting to locate the guest in the host.

The close contacts between the phenyl moiety of the guest g2 or g3 · HCl and the opening ring of the host TMeQ[6] show that the aromatic ring fits reasonably tightly in the cavity of the host. For example, carbon atoms of the benzene ring for both host-guest inclusion complexes lie between 3.34 Å and 4.50 Å from nearest-neighbour atoms in the host ring, with space-filling models showing that the ring fits reasonably tightly in the cavity. Thus, a combination of a hydrophobic interaction between the cavity of the TMeQ[6] and the phenyl moiety of g2 or g3 · HCl together with the hydrophilic interactions between a polar carbonyl portal group of TMeQ[6] and the positively charged imidazole of the guest was observed in these two inclusion complexes.

Conclusion

The ^{1}H NMR spectra analysis of the interaction of the four hosts cucurbit[n]urils Q[6–8] and a Q[6] derivative TMeQ[6] with three imidazole derivatives N-(4-hydroxylphenyl)imidazole (g1), N-(4-aminophenyl)imidazole (g2), and 2-phenylimidazole (g3) hydrochloride established two basic interaction models in which the host selectively binds the phenyl moiety of the title guests, forming inclusion complexes with a host:guest ratio of 1:1 for Q[6] or TMeQ[6] or Q[7] and a host:guest ratio of 1:2 for Q[8]. Relatively high formation constants in aqueous solution at pH 5.8 of logK values between 4 and 5 for the smaller Q[6 or 7]s, while logK values between 11 and 12 for Q[8] were determined through absorption and fluorescence spectroscopic analysis. The single crystal structure of the inclusion complex supports the solution studies, the inclusion complex assembled as identified in the solution ^{1}H NMR studies. The strength of the interaction determined here reflects the ability of cucurbit[n]urils to act as a host for suitably shaped guests, even in aqueous solution.

Acknowledgements Support of the National Natural Science Foundation of China (NSFC; No. 20662003 and 20767001), the "Chun-Hui" Funds of Chinese Ministry of Education, the Science and Technology Fund of Guizhou Province and the International Collaborative Project Fund of Guizhou province are gratefully acknowledged.

References

1. Day, A.I., Arnold, A.P., Blanch, R.J., Snushall, B.: Controlling factors in the synthesis of cucurbituril and its homologues. J. Org. Chem. **66**, 8094–8100 (2001). doi:10.1021/jo015897c
2. Kim, J., Jung, I.-S., Kim, S.-Y., Lee, E., Kang, J.-K., Sakamoto, S., Yamaguchi, K., Kim, K.: New cucurbituril homologues: syntheses, isolation, characterization, and X-ray crystal structures of cucurbit[n]uril ($n = 5$, 7, and 8). J. Am. Chem. Soc. **122**, 540–541 (2000). doi:10.1021/ja993376p
3. Day, A.I., Blanch, R.J., Arnold, A.P., Lorenzo, S., Lewis, G.R., Dance, I.: A cucurbituril-based gyroscane: a new supramolecular form. Angew. Chem. Int. Ed. Engl. **41**, 275–277 (2002). doi:10.1002/1521-3773(20020118)41:2<275::AID-ANIE275>3.0.CO;2-M
4. Lagona, J., Mukhopadhyay, P., Chakrabarti, S., Isaacs, L.: The cucurbit[n]uril family. Angew. Chem. Int. Ed **44**, 4844–4870 (2005). doi:10.1002/anie.200460675
5. Lee, J.W., Samal, S., Selvapalam, N., Kim, H.J., Kim, K.: Cucurbituril homologues and derivatives: new opportunities in supramolecular chemistry. Acc. Chem. Res. **36**, 621–630 (2003). doi:10.1021/ar020254k
6. Gerasko, O.A., Samsonenko, D.G., Fedin, V.P.: Supramolecular chemistry of cucurbituril. Russ. Chem. Rev. **71**, 741–760 (2002). doi:10.1070/RC2002v071n09ABEH000748
7. Elemans, J.A.A.W., Rowan, A.E., Nolte, R.J.M.: Self-assembled architectures from glycoluril. Ind. Eng. Chem. Res. **39**, 3419–3428 (2000). doi:10.1021/ie000079g
8. Hubin, T.J., Kolchinski, A.G., Vance, A.L., Busch, D.H.: Template control of supramolecular architecture. Adv. Supramol. Chem **5**, 237–357 (1999)
9. Mock, W.L.: Cucurbituril. Top. Curr. Chem **175**, 1–24 (1995)
10. Cintas, P.: Cucurbituril: supramolecular perspectives for an old ligand. J. Incl. Phenom. Mol. Reco. Chem. **17**, 205–220 (1994). doi:10.1007/BF00708781
11. Zhao, J.Z., Kim, H.J., Oh, J., Kim, S.Y., Lee, J., Sakamoto, W.S., Yamaguchi, K., Kim, K.: Cucurbit[n]uril derivatives soluble in water and organic solvents. Angew. Chem. Int. Ed. **40**, 4233–4235 (2001). doi:10.1002/1521-3773(20011119)40:22<4233::AID-ANIE4233>3.0.CO;2-D
12. Isobe, H., Sato, S., Nakamura, E.: Synthesis of disubstituted cucurbit[6]uril and its rotaxane derivative. Org. Lett. **4**, 1287–1289 (2002). doi:10.1021/ol025749o
13. Jon, S.Y., Selvapalam, N., Oh, D.H., Kang, J.K., Kim, S.Y., Jeon, Y.J., Lee, J.W., Kim, K.: Facile synthesis of cucurbit[n]uril derivatives via direct functionalization: expanding utilization of cucurbit[n]uril. J. Am. Chem. Soc. **125**, 10186–10187 (2003). doi:10.1021/ja036536c
14. Ma, P.-H., Xiao, X., Zhang, Y.-Q., Xue, S.-F., Tao, Z.: 1,3,5,7,9,11,13,15-Octaazapentacyclo [9.5.1.13,9.06,18.014,17] octadecane-4,8,12,16-tetrone monohydrate: a methylene-bridged glycoluril dimmer. Acta Cryst. **E64**, o1795 (2008)
15. Zhao, Y.-J., Xue, S.-F., Zhu, Q.-J., Tao, Z., Zhang, J.-X., Wei, Z.-B., Long, L.-S., Hu, M.-L., Xiao, H.-P., Day, A.I.: Synthesis of a symmetrical tetrasubstituted cucurbit[6]uril and its host-guest compound with 2,2′-bipyridine. Chin. Sci. Bull. **49**, 1111–1116 (2004). doi:10.1360/04wb0031
16. Zheng, L.-M., Zhu, J.-N., Zhang, Y.-Q., Tao, Z., Xue, S.-F., Zhu, Q.-J., Wei, Z.-B., Long, L.-S.: Synthesis and crystal structure of a novel self-assembled (1,4-discyclohexyl cucurbituril) sodium(I). complex. Chin. J. Inorg. Chem. **21**, 1583–1588 (2005)
17. Lu, L.-B., Yu, D.-H., Zhang, Y.-Q., Zhu, Q.-J., Xue, S.-F., Tao, Z.: Supramolecular assemblies based on some new methyl-substituted cucurbit[5]urils through hydrogen bonding. J. Mol. Struct. **885**, 70–75 (2008). doi:10.1016/j.molstruc.2007.10.008
18. Yu, D.-H., Ni, X.-L., Zhang, Y.-Q., Xue, S.-F., Zhu, Q.-J., Tao, Z.: Structures of supramolecular assemblies formed by some partial substituted cucurbiturils and some metal ion complexes. J. Mol. Struct. **882**, 128–133 (2008). doi:10.1016/j.molstruc.2007.09.025
19. Tian, Z.-C., Ni, X.-L., Xiao, X., Wu, F., Zhang, Y.-Q., Zhu, Q.-J., Xue, S.-F., Tao, Z.: Interaction models of three alkyl substituted cucurbit[6]urils with a hydrochloride salt of 4,4′-dipyridyl guest. J. Mol. Struct. **888**, 48–54 (2008). doi:10.1016/j.molstruc.2007.11.029
20. Ni, X.-L., Zhang, Y.-Q., Zhu, Q.-J., Xue, S.-F., Tao, Z.: Crystal structures of host–guest complexes of meta-tricyclohexyl cucurbit[6]uril with small organic molecules. J. Mol. Struct. **876**, 322–327 (2008). doi:10.1016/j.molstruc.2007.07.007
21. Lin, J.-X., Zhang, Y.-Q., Zhang, J.-X., Xue, S.-F., Zhu, Q.-J., Tao, Z.: Synthesis of partially methyl-substituted cucurbit[n]urils with 3a-methyl-glycoluril. J. Mol. Struct. **875**, 442–446 (2008). doi:10.1016/j.molstruc.2007.05.017
22. Ma, P.-H., Dong, J., Xiang, S.-C., Xue, S.-F., Zhu, Q.-J., Tao, Z., Zhang, J.-X., Zhou, X.: Interaction of host–guest complexes of cucurbit[n]urilswith double probe guests. Sci. China Ser. B **47**, 301–310 (2004). doi:10.1360/03yb0250
23. Liu, J.-X., Tao, Z., Xue, S.-F., Zhu, Q.-J., Zhang, J.-X.: Investigation of host–guest compounds of cucurbit[$n = 5$–8]uril with some piperazine derivatives. Chin. J. Inorg. Chem **20**, 139–146 (2003)
24. Zhao, Y.-J., Xue, S.-F., Zhu, Q.-J., Tao, Z., Zhang, Y.-Q., Zhang, J.-X., Wei, Z.-B., Long, L.-S.: Studies on the interaction of disubstituted cucurbit[6]uril with 2-(aminomethyl)pyridine. Acta Chim. Sinica **63**(10), 913–918 (2005)
25. Ma, P.-H., Tao, Z., Xue, S.-F., Zhu, Q.-J., Wang, S.-K., Yuan, S.-W., Zhang, J.-X., Zhou, X.: Interaction of cucurbit[n 6–8]urils with three N-benzyl cage guests. Chin. J. Org. Chem. **27**(3), 414–418 (2007)
26. Feng, Y., Xiao, X., Xue, S.-F., Zhang, Y.-Q., Zhu, Q.-J., Tao, Z., Lawrance, G.A., Wei, G.: Host–guest complex of a water soluble cucurbit[6]uril derivative with the hydrochloride salt of 3-amino-5-phenylpyrazole. Supramol. Chem. **20**(5), 517–525 (2008). doi:10.1080/10610270701457970
27. Huo, F.-J., Yin, C.-X., Yang, P.: The crystal structure, self-assembly, DNA-binding and cleavage studies of the [2]pseudorotaxane composed of cucurbit[6]uril. Bioorg. Med. Chem. Lett. **17**(4), 932–936 (2007). doi:10.1016/j.bmcl.2006.11.054
28. Sheldrick, G.M.: SHELXL97, Program for crystal structure determination. University of Göttingen, Germany (1997)
29. Fu, H.-Y., Xue, S.-F., Mu, L., Du, Y., Zhu, Q.-J., Tao, Z., Zhang, J.-X.: Host–guest complexes of cucubit[8]uril with phenanthrolines and its derivates. Sci. China Ser. B **48**(4), 305–314 (2005). doi:10.1360/04yb0072
30. Cong, H., Zhu, Q.-J., Hou, H.-B., Xue, S.-F., Tao, Z.: Interaction between cucurbit[8]uril and HCl salts of 3,4,7,8-tetramethyl-1, 10-phenanthroline. Supramol. Chem. **18**, 523–528 (2006). doi:10.1080/10610270600837181
31. Wu, M.-Q., Jiang, P.-Y., Fang, Z.-F., Xiao, X., Xue, S.-F., Zhu, Q.-J., Tao, Z.: Self-assembly modes of cucurbit[8]uril with bis(1,2,3,4-tetrahydroisoquinoline-2-ylmethyl). Acta Chim. Sinica **66**(18), 2081–2086 (2008)
32. Tao, Z., Zhu, Q.-J., Jackson, W.G., Zhou, Z.-Y., Zhou, X.-G.: On the preference for the sym-fac isomer in the [Co(N,N′-bis

(2-aminomethyl)amine)(2,2′-bipyridi- ne)Cl]$^{2+}$ system. Polyhedron **22**, 263–270 (2003). doi:10.1016/S0277-5387(02)01303-7

33. Zhu, Q.-J., Tao, Z., Zhang, J.-X., Zhang, G.-Y., Luo, X.-Q., Zhou, Z.-Y., Zhou, X.-G.: Assignment and configuration preference of a fac-isomer in the [Co(pema)(amp)Cl]$^{2+}$ system. Acta Chim. Sinica **61**, 729–735 (2003)
34. Lin, R.-G., Tao, Z., Xue, S.-F., Zhu, Q.-J., Jackson, W.G., Wei, Z.-B., Long, L.-S.: C–H···π interactions in the [Co(N-(2-pyridylmethyl)-1,3-diaminopropane) (2-aminomethylpyridine) Cl]$^{2+}$ system: syntheses, 2D-NMR, X-Ray structures and energy minimisations. Polyhedron **22**, 3467–3474 (2003). doi:10.1016/S0277-5387(03)00429-7
35. Tao, Z., Zhang, G.-Y., Luo, X.-Q., Xue, S.-F., Zhu, Q.-J., Jackson, W.G., Wei, Z.-B., Long, L.-S.: C-H···π Interactions in the [Co(N-(2-aminomethylpyridyl)ethylenediamine)(2-aminomethylpyridine) Cl]$^{2+}$ system: syntheses, 2D-NMR, X-ray structures and energy minimisations. Inorg. Chim. Acta **357**, 953–964 (2004). doi:10.1016/j.ica.2003.12.032